arXiv:2202.00630v2 [physics.soc-ph] 15 Apr 2022

OPINION DYNAMICS RELATED TO COVID-19 VACCINE HESITANCY AND MEGA-INFLUENCERS

ANNA HAENSCH, NATASA DRAGOVIC, CHRISTOPH BÖRGERS, AND BRUCE BOGHOSIAN

Abstract. Covid-19 vaccines are widely available in the United States, yet our Covid-19 vaccination rates have remained far below 100%. Data from the CDC show that even in places where vaccine acceptance was proportionally high at the outset of the Covid-19 vaccination effort, that willingness has not necessarily translated into high rates of vaccination over the subsequent months. We model how such a shift could have arisen, using parameters in agreement with data from the state of Alabama. The simulations suggest that in Alabama, local interactions would have favored the emergence of tight consensus around the initial majority view, which was to accept the Covid-19 vaccine. Yet this is not what happened. We therefore add to our model the impact of mega-influencers such as mass media, the governor of the state, etc. Our simulations show that a single vaccine-hesitant mega-influencer, reaching a large fraction of the population, can indeed cause the consensus to shift radically, from acceptance to hesitancy. Surprisingly this is true even when the mega-influencer only reaches individuals who are already somewhat inclined to agree with them, and under the conservative assumption that individuals give no more weight to the mega-influencer than they would give to a single one of their friends or neighbors. Our simulations also suggest that a competing mega-influencer with the opposite view *can* shift the mean population opinion back, but under some conditions *cannot* restore the tightness of consensus around that view. Our code and data are distributed in the ODyN (Opinion Dynamic Networks) library available at https://github.com/annahaensch/ODyN.

1. Introduction

Opinions drive human behavior [1], and opinion formation is a complex multi-scale process, involving characteristics of the individual, local interaction of individuals, social media, mass media etc. Opinion dynamics have been modeled using approaches inspired by physics [2]. A survey of the literature on opinion dynamics can be found in [3]. In this study, we use the example of opinions about Covid-19 vaccination, in part because the topic is of urgent current interest, but also because data are plentiful (see for instance [4], which we use as a source in our simulations), and a significant shift in opinions appears to have occurred in the United States in a short time span. We focus on two scales, local interactions (conversations with friends, family, neighbors, colleagues) and global influencers such as mass media and prominent politicians, whom we refer to as *mega-influencers*. Social media can belong to either category. A discussion of the merits or perils of Covid-19 vaccination among 25 Facebook friends could be viewed as a local interaction, whereas a Twitter account owner with millions of followers is a mega-influencer. In the model of this paper, social media will not appear explicitly. Despite the apparent geography-less nature of the online world, studies have shown [5] that geographic distance is still a key component in the formation and maintenance of social networks. Therefore, in the present paper we situate individuals in physical and opinion distance, and take this as a model for our network.

Date: 8 April 2022.

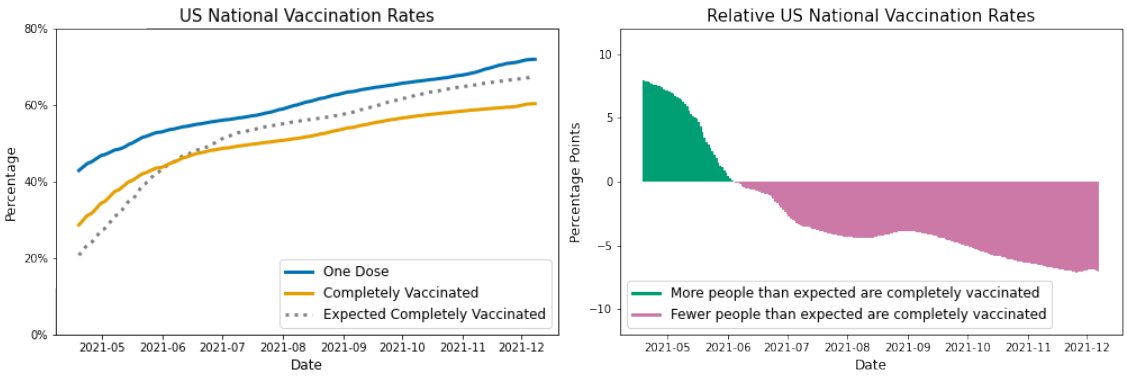


FIGURE 1. Left: U.S. national vaccination rates. "Completely vaccinated" means one dose of Johnson & Johnson or two doses of Pfizer/BioNTech or Moderna. "Expected completely vaccinated" curve obtained by shifting "one dose" curve forward by 42 days. Right: Actual minus expected vaccination rates.

Covid-19 vaccination rates over time have been closely tracked by the US Centers for Disease Control and Prevention at both the national and county levels [4, 6, 7, 8]. By April 19, 2021, vaccination was approved for everyone in the US age 16 and older. Despite the fact that the vaccine was free to all residents of the US, many factors impeded widespread vaccination. There was a lack of availability and access to vaccines in rural areas [9], social and economic factors impacted vaccine hesitancy [10], and there were also targeted misinformation campaigns and politicization of issues surrounding the vaccine [11]. Fear of adverse health effects related to the Covid vaccine might also be factor, despite the fact that studies have shown that adverse effects are quite rare [12]. For purposes of this study, we intend to focus entirely on the social dynamics of vaccine hesitancy as one possible explanation for vaccination levels lagging below what is expected.

Fig 1 shows the proportion of *partially* vaccinated people in the US as a function of time, beginning on April 19, 2021 (blue), and also the proportion of *fully* vaccinated people (orange). The proportion of fully vaccinated people around December of 2021 was around 60%. According to the terminology introduced by the CDC and widely adopted throughout Covid related news coverate, a person is considered *fully vaccinated* if they have had either one shot of the Johnson & Johnson vaccine or two shots of the Pfizer/BioNTech or Moderna vaccine, where the second shot must follow within 42 days of the first [13]. Fig 1 also shows that the actual number of people who achieved complete vaccination at some point began to fall short of the expected number. In other words, despite having access to the vaccine, and receiving their first dose, people did not always follow through with their second dose (orange in Fig 1). There appears to have been a shift towards greater vaccine hesitancy over time. Similar trends can be seen at the county level, in many counties throughout the United States (Fig 2). In this paper we examine how such a shift might have come about.

Opinions about issues such as Covid-19 vaccination are formed in part by people talking to their families, friends, colleagues, etc. This is the sort of mechanism that for instance the Hegselmann-Krause (bounded confidence) model [14] aims to capture. In [15], Hegeselmann and Krause modify their model further to consider the impact of radicals on opinions. In their model, radicals are individuals (or groups of individuals) that hold extreme and persistent

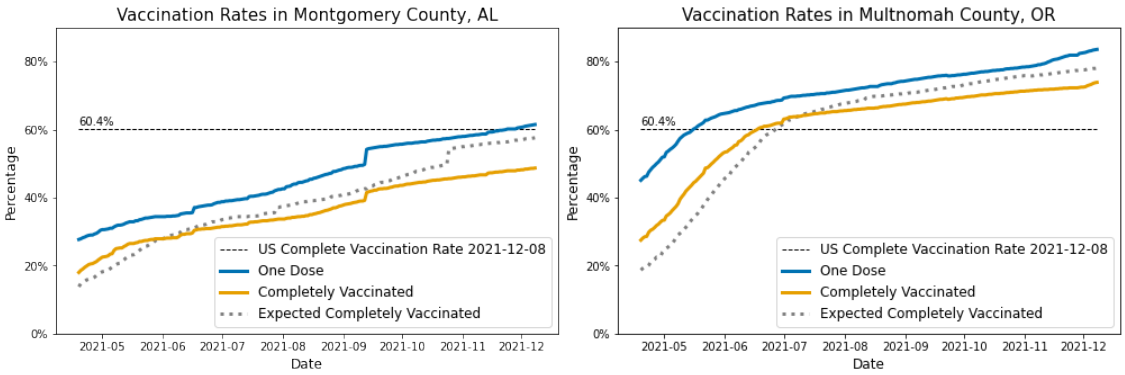


FIGURE 2. The vaccination rate is below the national average in Montgomery County, AL (left), above it in Multnomah County, OR (right). Yet in both counties, a shift towards greater hesitancy appears to have occurred, indicated by the fact that the orange curves have fallen below the dotted grey ones.

opinions on a single end of the opinion spectrum. By contrast, our model aims to capture geospatial as well as opinion space dynamics in the presence of what we've called *mega-influencers* on both ends of the spectrum. We endeavor to explore how *mega-influencers* such as mass media and prominent politicians interact with Hegselmann-Krause-type dynamics.

We define a random graph in which the vertices represent individuals, and *directed* edges indicate who influences whom. (When individual v's opinion influences that of individual u, this does not necessarily imply that u also influences v.) In our model, different people have different levels of influence, as in a Chung-Lu random graph [16, 17, 18]. Further, in our model people are more likely to be connected to those who are spatially closer to them, as in the geometric inhomogeneous random graphs of Brigmann *et al.* [19]. As in work by Mathias et al. [20] we include the influence of a small number of individuals holding extreme, immutable beliefs, we call them *mega-influencers* (related literature also uses the term *radicals*). Our treatment differs from [20] in that the underlying network is spatial and mimics a real word network (see Section 4 for a more robust discussion on the network parameters). For a review of spatial networks, we direct the reader to Barthélemy's comprehensive survey on the topic [21]. The networks that we propose in the present paper are similar to the hidden variable model for spatial networks presented in [21, Section 3], but futher enhanced to include bounded confidence.

To initialize the network model every person starts with their own *belief*, defined as their position in opinion space, and individual beliefs evolve according to the Hegselmann-Krause model [14], which assumes that people are influenced only by opinions similar to theirs. The Hegselmann-Krause model has been studied extensively in the literature [22, 23, 24, 25]. It is just one of several popular opinion dynamics models; see [26, 27, 28, 29] for other examples.

In the simulations presented here, the spatial domain is a triangle, and the spatial locations of individuals are independent of each other and uniformly distributed. The code in the ODyN (Opinion Dynamic Networks) library (`https://github.com/annahaensch/ODyN`) also allows simulations on unions of triangles, where the number of individuals in each triangle is chosen to be random, Poisson-distributed, with an expected value proportional to

the area of the triangle, possibly with different constants of proportionality for different triangles. In short, the spatial locations in the ODyN library are a Poisson point process with a possibly space-dependent rate. We plan to use this code to study irregular shapes such as US states by (approximate) triangulation in the future; see Fig 3.

Simulations of our model suggest that in Alabama, local interactions would have favored consensus around the initial majority view, which was to accept the Covid vaccine. We show that the addition of a vaccine-hesitant mega-influencer can cause the consensus to shift radically, from acceptance to hesitancy. A competing mega-influencer with the opposite view can bring the mean of the opinion distribution back, but the spread of opinions will be significantly greater with both mega-influencers present than without either of them. Our code and data are distributed in the ODyN library.

2. Model

2.1. **Directed graph encoding who influences whom.** Let N be a positive integer, and consider N individuals. We use letters such as u and v (for "vertex"), $1 \leq u, v \leq N$, to label individuals. We will construct a random *directed* graph in which the individuals are the vertices, with an arrow (a directed edge) from individual v to individual u indicating that v influences the opinion of u. We write

$$p_{uv} = \text{probability of an arrow from } v \text{ to } u.$$

We do not assume symmetry: p_{vu} need not be equal to p_{uv}.

2.2. **Spatial locations.** This part of our model is inspired by [19], although several of the details are different here. We assign to individual v a random spatial location X_v in a polygonal domain D in the plane. In the code available through ODyN, D is assumed to be a union of triangles, and the number of individuals per triangle is taken to be random with Poisson distribution, with a rate that can be different for different triangles. The locations of individuals within each triangle are then assumed to be independent and random with uniform distribution (see Fig 3 for an example). We use triangles because they are a flexible way of approximating more complicated shapes, and it is straightforward to generate uniformly distributed random points in a triangle.

In the simulations presented here, we simply take D to be a single triangle, fix N, and let the locations $X_1, X_2, \ldots, X_N$ of the individuals be independent, uniformly distributed points in D. We assume that p_{uv} is a decreasing function of the euclidean distance $\|X_u - X_v\|$.

2.3. **Influence weights.** Following Chung and Lu [16], we assign a random *influence weight* $W_v > 0$ to each v. This weight determines how likely others are to listen to v, not how much weight they assign to v's opinion; the probability p_{uv} is an increasing function of W_v.

We assume W_v to be a heavy-tailed random variable that is always greater than 1. Specifically, we assume that for any $x > 1$,

$$P(W_v > x) = \frac{1}{x^\gamma}, \tag{1}$$

with some exponent $\gamma > 0$. (The parameter β of [16] is $\gamma + 1$.) To generate a random number W_v with the complementary distribution function (1), draw a uniformly distributed random number $U \in (0, 1)$, then set

$$W_v = U^{-\frac{1}{\gamma}}.$$

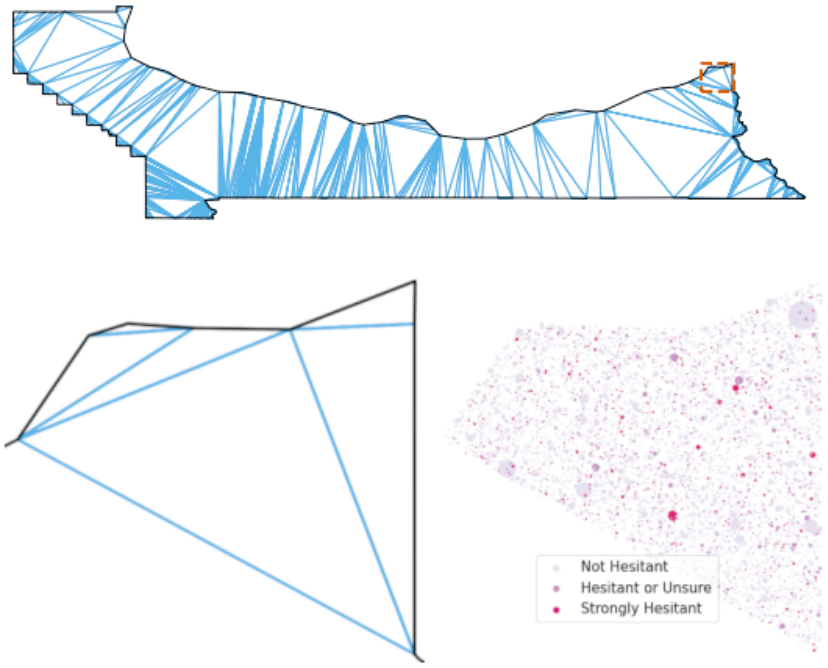


FIGURE 3. The polygonal boundary of Multnomah County, Oregon (top) is triangulated prior to populating with a Poisson point process. Triangular regions (bottom left) are populated with the proper population density and belief proportion (bottom right). Triangles are generated to connect all vertices on the polygonal region that represents the county geometry. In some cases boundary points appear colinear at this resolution, although in reality they are not.

We will choose a value of γ that makes the mean of the distribution of the W_v finite: $\gamma > 1$. Given this constraint, however, we will choose γ to make the variance of the distribution infinite, so that outlying values of W_v become fairly common. The variance is infinite for $1 < \gamma \leq 2$, and since within this range, we don't expect the precise value of γ to have a qualitative impact on our results, we choose $\gamma = 1.5$.

2.4. **Opinion scores.** We assign to each individual v an *opinion score* H_v between 0 and 2, reflecting their view on Covid-19 vaccines, ranging from $H_v = 0$ (no hesitancy) to $H_v = 2$ (strong hesitancy). We assume that $p_{uv} = 0$ if $|H_u - H_v| \geq b$, where $b > 0$ is a threshold. That is, we assume that v cannot have any impact on u's opinion if u and v have starkly different views.

2.5. **Overall formula for the connection probabilities.** We define

$$p_{uv} = \min\left(1, \frac{1}{(1 + \|X_u - X_v\|/\lambda)^{\delta}} \, W_v^{\alpha} \, \mathbb{1}_{|H_u - H_v| < b}\right) \tag{2}$$

where $\mathbb{1}$ denotes the indicator function. The parameter $\lambda > 0$ is a reference length; we take it to be the diameter of the spatial domain. The parameters $\alpha > 0$ and $\delta > 0$ determine the importance of influence weight and spatial proximity, respectively.

2.6. **Initialization.** The influence weights W_u and spatial locations X_u are independent random numbers, chosen as outlined above. The opinion scores H_u change with time; see Section 2.7. We assign a random initial opinon score to each individual u. These assignments are made independently of each other, and independently of the H_u and W_u. Initial opinion scores take on integer values only: 0, 1, or 2. The probability that an individual u is assigned the initial opinion score k equals p_k, $k = 0, 1, 2$, where the p_k are chosen to reflect publicly available data. At later times, we allow the H_u to take on any values in the interval $[0, 2]$.

2.7. **Hegselmann-Krause dynamics.** Denote the opinion scores after t time steps by $H_u(t)$. (We take t to be a non-negative integer here.) Then $H_u(t)$ is the average of those $H_v(t-1)$ for which either $v = u$, or there is an arrow pointing from v to u at time $t-1$. In words, u averages their own opinion with the opinions of those whom u is influenced by. This is the Hegselmann-Krause model [14].

Since the probabilities p_{uv} depend on $H_u - H_v$, they, too, are time-dependent. The connections in the random graph are re-drawn after each time step. The motivation for re-drawing the connections after each timestep is to simulate the fact that people don't necessarily speak and interact with the same people every day.

2.8. **In-degree and clustering coefficient.** The in-degree of an individual u is the number of individuals v who influence u, that is, the number of v for which there is an arrow from v to u. We will keep track of the average in-degree. As the graph is time-dependent, so is the average in-degree. Since every outgoing arrow for one vertex is an incoming arrow for another vertex, the average in-degree is the same as the average out-degree.

The *clustering coefficient* of an individual u is defined as follows. Denote by k the number of individuals who influence u. If $k \leq 1$, then u has clustering coefficient 0. Otherwise, determine for each of the $k(k-1)$ ordered pairs of individuals who influence u whether it is connected, that is, whether there is an arrow from the first to the second. The fraction of connected pairs is the clustering coefficient of u.

Both the average in-degree and the average clustering coefficient provide a way of evaluating whether our graphs are realistic, and therefore help in setting parameters. The average in-degree should not be unrealistically high or low, and the average clustering coefficient should not be too low. To see the overall effect of the inclusion of weights and beliefs on the clustering coefficients and in-degree, we have initialized several populations varying components informing the probability of adjacency (i.e. opinions, weights, or both), see Fig 4. The network model we work with is on the bottom right of Fig 4.

2.9. **Mega-influencers.** We add to the model two *mega-influencers*, one with opinion score 0, referred to as the *left mega-influencer*, and the other with opinion score 2, the *right mega-influencer*. One might think of these as modeling mass media outlets, outspoken governors, etc.

The impact of the mega-influencers is modeled as follows. To each individual u, we assign two random numbers L_u and R_u, with

$$L_u = \begin{cases} 1 & \text{with probability } p_L, \\ 0 & \text{otherwise,} \end{cases} \qquad \text{and} \qquad R_u = \begin{cases} 1 & \text{with probability } p_R, \\ 0 & \text{otherwise,} \end{cases}$$

where p_L and p_R are further model parameters, with $0 \leq p_L, p_R \leq 1$. If $L_u = 1$, then u is susceptible to the left mega-influencer. In that case, while $H_u \in [0, \epsilon)$, where $\epsilon > 0$ is another mode parameter, the opinion score of the left mega-influencer, namely 0, will

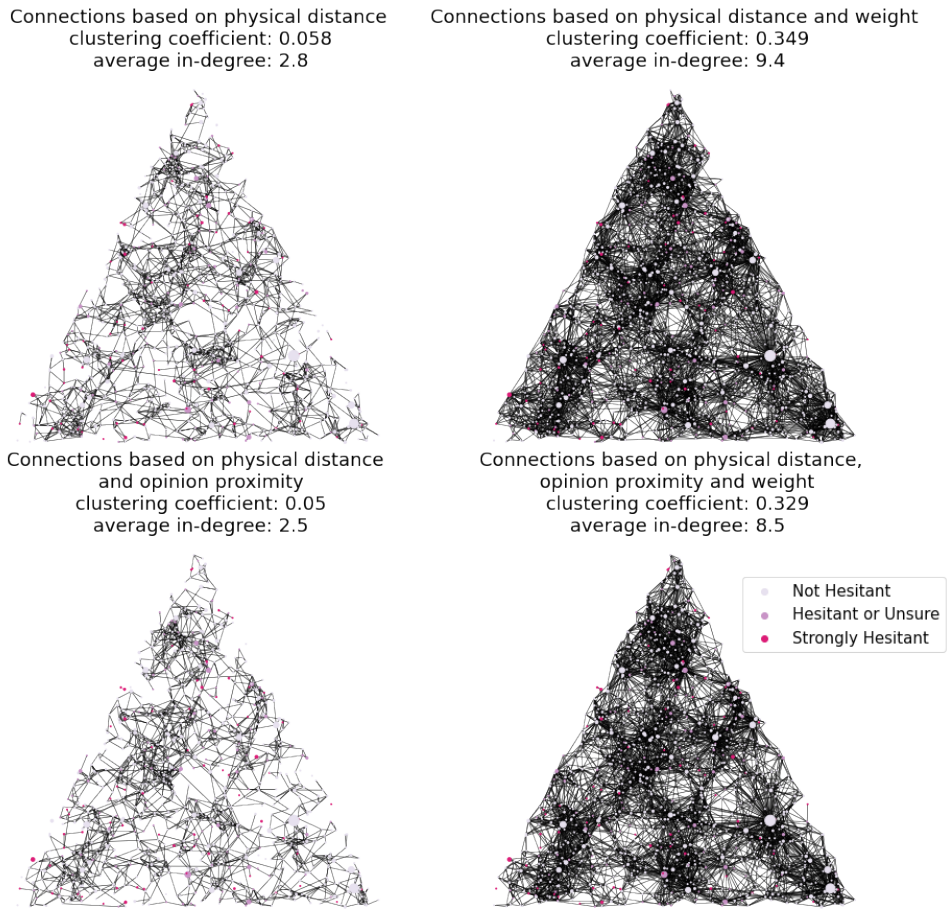


FIGURE 4. Four different initialized network model with $n = 1000$ individuals, symmetric initial beliefs and varying active components informing the probability of adjacency. The initialization on the lower right is the one we actually use in our experiments.

be added to the opinions over which u averages in each step of the Hegselmann-Krause dynamics. Similarly, if $R_u = 1$, then u is susceptible to the right mega-influencer. In that case, while $H_u \in (2 - \epsilon, 2]$, the opinion score of the right mega-influencer, namely 2, will be added to the opinions over which u averages in each step. The parameters b and ϵ play similar roles, for local interactions and for mega-influencers, respectively. In the code, they need not be the same, but in the simulations presented here, they were the same.

Note that our model assumes that to u, mega-influencers do not carry more weight than friends or neighbors. The very considerable effect of mega-influencers that we will demonstrate in the computational results is all the more surprising.

2.10. **Parameterization and Model Creation.** The parameters in our model are n, λ, γ, δ, α, b, ϵ, p_L, and p_R. Using the ODyN library, the `OpionionNetworkModel` class can be initialized with these parameters as arguments. This model can be populated with individuals bearing both weight and belief scores as described in the previous sections using `populate_model()`. The belief propagation simulator is loaded as a separate class, `NetworkSimulator,` and network simulations can be carried out on the model with

`run_simulation()`. Further documentation and demonstrations of this workflow can be found on the project Github page, and pseudocode for these procedures are given in Algorithms 1 and 2 below.

3. Data Overview

3.1. **CDC Vaccine Rate Data.** The Centers for Disease Control (CDC) vaccine trends data set shows overall trends in vaccination at the county level [6]. This data set includes counts and per-capita rates of first dose administration and full vaccination. For more comprehensive information about the data reporting see [8]. The most current version of this data set can be loaded into ODyN using the function `load_county_trend_data` with the argument `download_data = True`. This will pull the most up-to-date county vaccination data directly from the CDC website.

3.2. **ASPE Vaccine Hesitancy Data.** The Assistant Secretary for Planning and Evaluation (ASPE) vaccine hesitancy data set gives county level estimates for Covid-19 vaccine hesitancy [4]. State level estimates of vaccine hesitancy from the 2019 Household Pulse Survey (HPS) are combined with the Census Bureau's 2019 American Community Survey (ACS) 1-year Public Use Microdata Sample (PUMS) to obtain county level estimates of Covid-19 vaccine hesitancy. The HPS includes the survey question: *"Once a vaccine to prevent Covid-19 is available to you, would you...get a vaccine?"*, with the responses 1) "definitely get a vaccine", 2) "probably get a vaccine", 3) "unsure", 4) "probably not get a vaccine" and 5) "definitely not get a vaccine." In the results of this survey, responses are reduced to a 3-point scale, classified as,

- *Strongly hesitant* if "definitely not."
- *Hesitant or unsure* if "unsure" or "probably not" or "definitely not."

We assign a belief score of 2 to the "strongly hesitant," a belief score of 1 to those who are "hesitant or unsure" but not "strongly hesitant," and a belief score of 0 to all others. In this work we adopt the language and 3-point scale classification, since the raw data (i.e. 5-point) responses are not made available. We use HPS data from Week 31, i.e., May 26, 2021 to June 7, 2021 [30]. This data set can be loaded into ODyN using the function `load_county_hesitancy_data` with the argument `download_data = True`. This will load the Week 31 hesitancy data set directory from the CDC website. Earlier data sets documenting vaccine hesitancy exist and have been used to examine trends in hesitancy at the county level [31]. However, the CDC survey methodology changed, so older data are not comparable to Week 31 data.

4. Experimental Methodology

The model described in Section 2 is generated by Algorithms 1 and 2 below. To populate the network, we generate uniformly distributed random points in a triangle T.

4.1. **Exploration of parameter space.** We run several experiments varying initial belief distributions, as well as the reach of influence from the left and right. Each of the experiments has $n = 1000$ agents/vertices and parameters: $\lambda = 1/10$ the diameter of T, $\delta = 8.5$, $\alpha = 1.6$, $b = 1.5$ and $\epsilon = 1.5$. These parameters were explicitly chosen to achieve clustering coefficients and in-degrees that were realistic for real-life community interactions, namely, a consistent clustering coefficient of approximately 0.3 as well as an average in-degree between

Algorithm 1

procedure `populate_model`(n,T, γ, (p_0, p_1, p_2), λ,α, b, ϵ, p_L, p_R)
  $t_1, t_2, t_3 \leftarrow$ vertices of triangle T.
  `Agent` $\leftarrow$ empty $n \times 2$ position array
  `Weight` $\leftarrow$ empty $n \times 1$ weight array
  `Neighbor` $\leftarrow$ $n \times n$ array of zeros.
  `MegaInfluences` $\leftarrow$ empty $n \times 2$ array.
  for $i \leq n$ **do**
    $x, y, w \leftarrow$ sampled from $U(0, 1)$
    if $x + y > 1$ is even **then**
      $x \leftarrow 1 - x$
      $y \leftarrow 1 - y$
    end if
    `Agent`$[i] \leftarrow x \cdot (t_2 - t_1) + y \cdot (t_3 - t_1)$
    `Weight`$[i] \leftarrow$sampled from $U(0, 1)$
  end for
  `Weight` $\leftarrow$ `Weight`$^{-\frac{1}{\gamma}}$
  `Belief` $\leftarrow n \times 1$ array sampled from $[0, 1, 2]$ with probabilities (p_0, p_1, p_2), resp.
  for $i \leq n$ **do**
    for $j \leq n$ with $i \neq j$ **do**
      $x \leftarrow$ sampled from $U(0, 1)$
      if $x < p_{u_i u_j}$ computed using Eq (2) **then**
        `Neighbor`$[i, j] \leftarrow 1$
      end if
    end for
  end for
  $L \leftarrow$ set of agents with belief within ϵ of the left influencer.
  $R \leftarrow$ set of agents with belief within ϵ of the right influencer.
  for i in randomly sampled subset of L with size $p_L \cdot \mid L \mid$ **do**
    `MegaInfluencer`$[i, 0] \leftarrow 1$
  end for
  for i in randomly sampled subset of R with size $p_R \cdot \mid R \mid$ **do**
    `MegaInfluencer`$[i, 1] \leftarrow 1$
  end for
  return `Agent`, `Weight`, `Belief`, `Neighbor`, `MegaInfluencer`
end procedure

7 and 9 (for populations that begin with a strong consensus belief, we expect marginally higher average degree). Though a person might interact with a larger number of individuals through their online social networks, or a smaller number of individuals through in-person interactions, surveys have shown that people report feeling genuinely close to between 5 and 10 individuals in their social circle, broadly construed [32]. The clustering coefficient was chosen to be consistent with values for average clustering coefficients on directed graphs using random walks on social networks [33]. As noted earlier, when generating the weights W_u, we used $\gamma = 1.5$ which yields a heavy-tailed distribution that has finite mean but infinite variance. Due to computational constraints, in the present paper we do not carry out a full

exploration of parameter space, although this is an interesting next step in the research. But our limited selection of parameters were chosen to mimic a real-life network in a way that's quantitatively supported by social science research as mentioed above. Similary we restrict our attention to networks with only 1000 nodes, bearing in mind that such networks may be susceptible to edge effects.

Algorithm 2

procedure `run_simulation`(n,Δ, γ, (p_0, p_1, p_2), λ,α, b, ϵ, p_L, p_R)
  Compute `Agent`, `Weight`, `Belief`, `Neighbor`, `MegaInfluencer` with Algorithm 1.
  while `True` **do**
    for $j \leq n$ **do**
      $S \leftarrow \{\texttt{Belief}[j]\} \cup \{\texttt{Belief}[k] : \texttt{Neighbor}[k, j] = 1 \text{ for } k \neq j\}$
      if `MegaInfluencer`$[j, 0] = 1$ **then**
        if `Belief`$[j] < \epsilon$ **then**
          # Include left mega-influencer belief in S.
          $S \leftarrow S \cup \{\text{left mega-influencer belief (i.e. } 0)\}$
        else
          # Connect to right mega-influencer with probability p_R.
          $x \leftarrow$ sampled from $U(0, 1)$
          if $x < p_R$ **then**
            `MegaInfluencer`$[j, 0] \leftarrow 0$ and `MegaInfluencer`$[j, 1] \leftarrow 1$
          end if
        end if
      end if
      Repeat steps 6 - 17 for right mega influencer.
      # Propagate all local beliefs.
      `Belief`$[j] \leftarrow$ average of beliefs in S.
    end for
    # Recompute network graph using updated beliefs.
    `Neighbor` $\leftarrow$ Recompute `Neighbor` using steps 18 - 25 in Algorithm 1.
    if `stopping_criterion_satisfied` **then**
      `break`
    end if
  end while
  return `Belief`
end procedure

As our initial belief distributions, we consider four distinct cases as shown in Table 1. For the *Vaccine Accepting* population we use the initial hesitancy beliefs of Multnomah County, Oregon, and we negate these beliefs to seed a *Vaccine Skeptical* population. The *Skewed* beliefs are distributed according to the vaccine hesitancy beliefs in Montgomery County, Alabama, which skew towards acceptance, but with a significant skeptical population. Finally, we include a fictitious population with *Symmetric* beliefs to demonstrate the outcomes in a symmetric population. Using these distributions, we seed our model using Algorithm 1 to obtain the initial network models shown in Fig 6.

With Algorithm 1 we assign attributes to individual agents such as weight, spatial distance, position in opinion space, and connection to mega-influencers, which we then use to compute

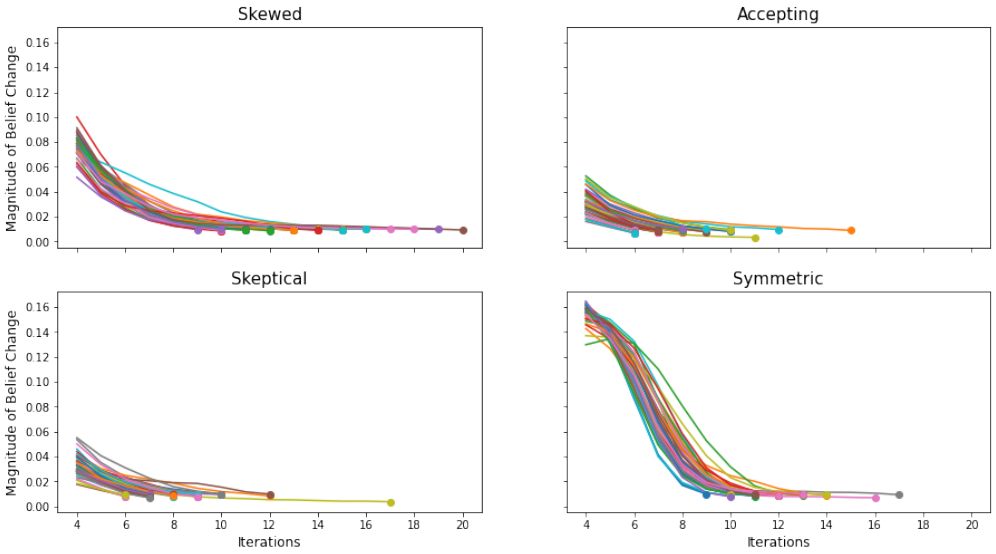


FIGURE 5. Mean change in absolute belief over timesteps. The simulation is stopped when the community-wide mean of absolute change in belief drops below a .01 across a 5-time step rolling average.

the network graph. Using Algorithm 2 we synchronously update all opinions. After each round of opinion updates, the network graph is recomputed holding weight and spatial distance parameters constant.

4.2. **Stopping criterion.** For each initial belief distribution, we carry out seven experiments, using Algorithm 2, varying the left and right mega-influence (i.e., varying p_L and p_R). In one experiment we set both of p_L and p_R equal to 0 to simulate a population without any influence from mega-influencers. In the remaining six experiments, $p_R = 0.8$ and $p_L = 0, .2, .4, .6, .8$ or 1. A stopping criterion is determined as follows. At each timestep, a 5-time step rolling average in belief change is calculated for each individual. The community-wide mean of the absolute change in belief is then computed. When this value drops below .01, the simulation is stopped. We note that this allows for individuals to have small oscilations in opinion, but overall the community opinion stabilizes. For brevity, in Algorithm 2 we indicate this with a boolean `stopping_criterion_satisfied`. In Fig 5, we can see that this threshold is typically reached in 20 or fewer time steps.

After each time step the network adjacencies are re-computed according to the updated beliefs. This reflects the fact that somebody who influences my opinion today may not influence it tomorrow, for instance because I may happen not to talk to them tomorrow. Fig 6 depicts examples of the initialized networks for each of the four scenarios we analyzed. For each of the scenarios the average-in degree was between 6 and 9, which corresponds to realistic social networks [32, 33]. Our simulation results are presented in Section 5.

5. RESULTS

We visualize our simulations using smoothed ridge plots with a Gaussian kernel density estimate. Results with $p_L = 0$ and $p_R = 0$ (no mega-influencers) are shown in Fig 7. We

Belief Type	p_0	p_1	p_2	Mean Belief	Corresponding US County
Vaccine Accepting	0.8831	0.0492	0.0677	0.1846	Multnomah County, OR
Vaccine Skeptical	0.0677	0.0492	0.8831	1.8154	
Skewed	0.7877	0.0988	0.1135	0.3258	Montgomery County, AL
Symmetric	0.4500	0.1000	0.4500	1.0000	

TABLE 1. Initial Population Belief Distributions

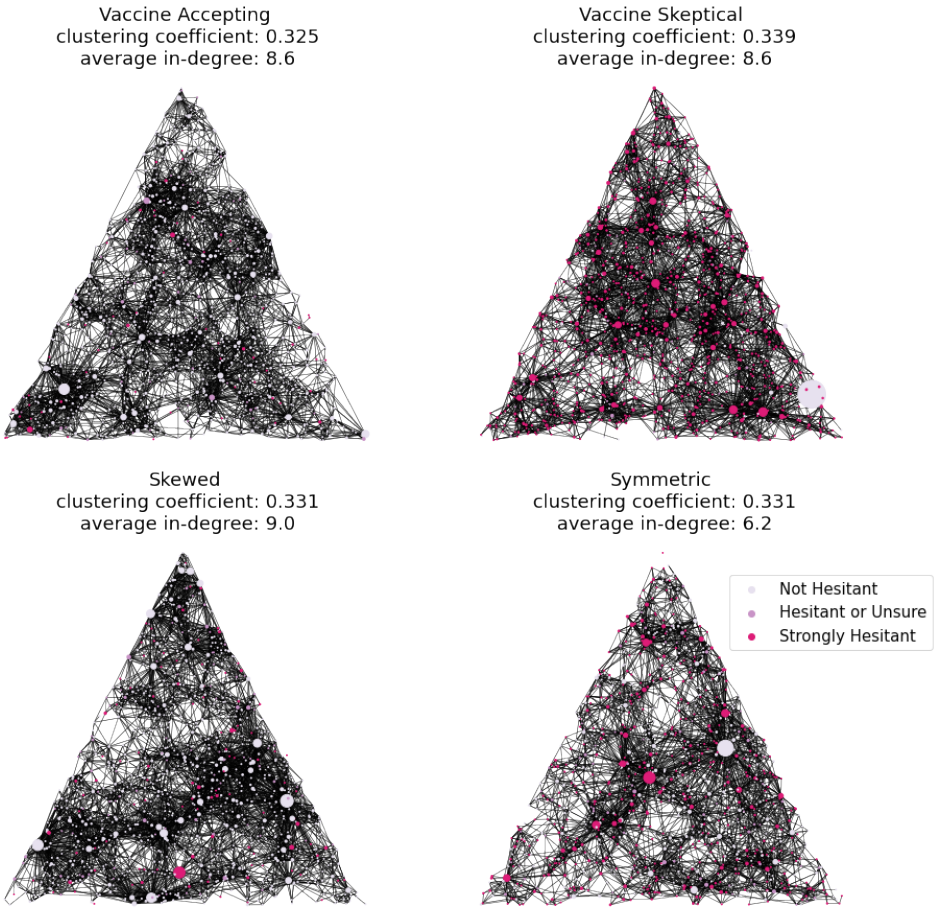


FIGURE 6. Initialized networks with varying initial belief distributions from Table 1, for $n = 1000$ individuals and connections based on weight and distance in both physical and opinion space.

see that without mega-influencers, populations tend to reach tight consensus near the mean of the initial opinion distribution. For clarity and ease of comparison, in this section we show the results for one simulation that was carried for precisely 60 timesteps (well beyond the stopping criterion for all scenarios); these artificially truncated simulations still provide statistically sound examples of the the overall trends from all simulations, which is further confirmed by the aggregate statistics presented in Fig 12. In Hegselmann-Krause dynamics, often multiple clusters are seen, not just a single peak [14]. In our simulations, we invariably see a single peak forming. This is because we use a fairly large value of the parameter b;

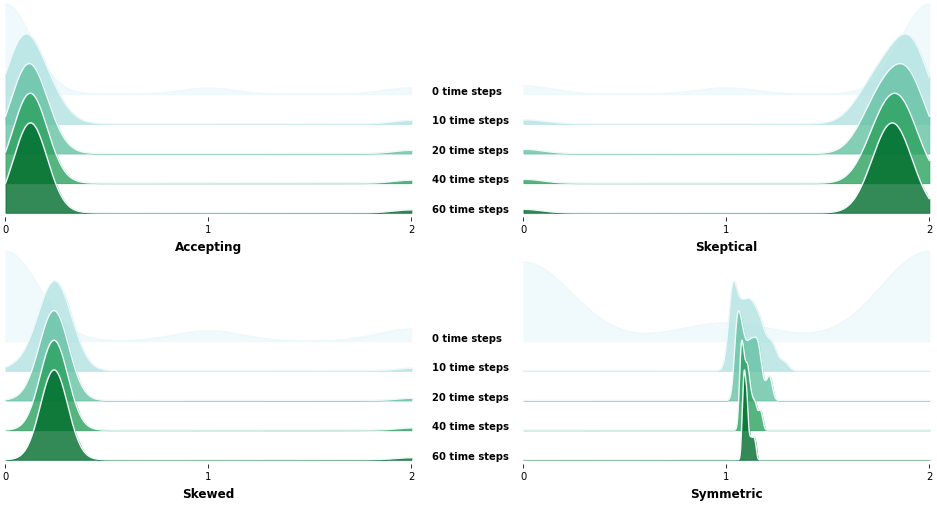


FIGURE 7. Populations with initial belief distributions from Table 1 over 60 time steps without mega-influencers.

that is, in our model, people are fairly willing to listen to others with somewhat diverging views, and be influenced by those views.

Now we set p_R (the reach of the right influencer) to 80% and vary the reach of the left influencer to see how this impacts the long term opinions of variously seeded populations. These results are shown for the Vaccine Accepting (Fig 8), Vaccine Skeptical (Fig 9), Skewed (Fig 10), and Symmetric (Fig 11).

In the Vaccine Accepting population, we see that even in the absence of mega-influence from the left, the population remains relatively vaccine accepting over 60 time steps although there is some diffusion of opinion. With a modest increase of 20% reach by the left mega-influencers, vaccine acceptance remains the dominating consensus belief. Unsurprisingly, the equivalent but opposite behavior is witnessed in the Vaccine Skeptical population. Of course there is slight variance in the two outcomes due to the stochastic nature of the simulation.

This behavior is summarized in Fig 12, which shows an average across 50 runs of the mean belief at stopping, where the left influencer's reach is changing but the right one is kept at 80% reach. In a vaccine skeptical population, given sufficient mega-influence from the right, no amount of left influence is capable of changing vaccine beliefs in any meaningful way. However, critically, we see that in skewed populations (such as we see in Mongtomery County, AL) a change in left influence has a dramatic impact on the overall vaccine acceptance rate. With a left influencer reach of 60% the mean belief is around 0.25 which suggests a willingness to receive a vaccine.

The experiments can be easily replicated in the command line with scripts included in ODyN: `accepting_simulation.py`, `skeptical_simulation.py`, `symmetric_simulation.py` and `skewed_simulation.py`. The data corresponding to these results is stored on Github at https://github.com/annahaensch/ODyN/tree/main/data/simulations_from_paper and the ODyN repository also includes a Jupyter notebook to recreate the plots shown in this paper.

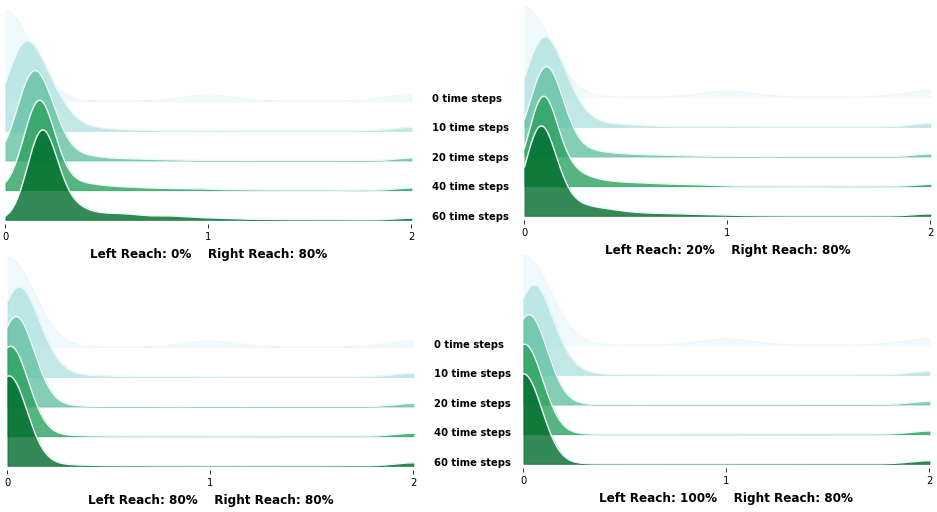


FIGURE 8. A population with *accepting* initial beliefs (such as Multnomah County, Oregon) over 60 time steps with a right mega-influencer of strong reach ($p_R = 0.8$) and a left mega-influencer of varying reach ($p_L = 0, 0.2, 0.8$,and 1).

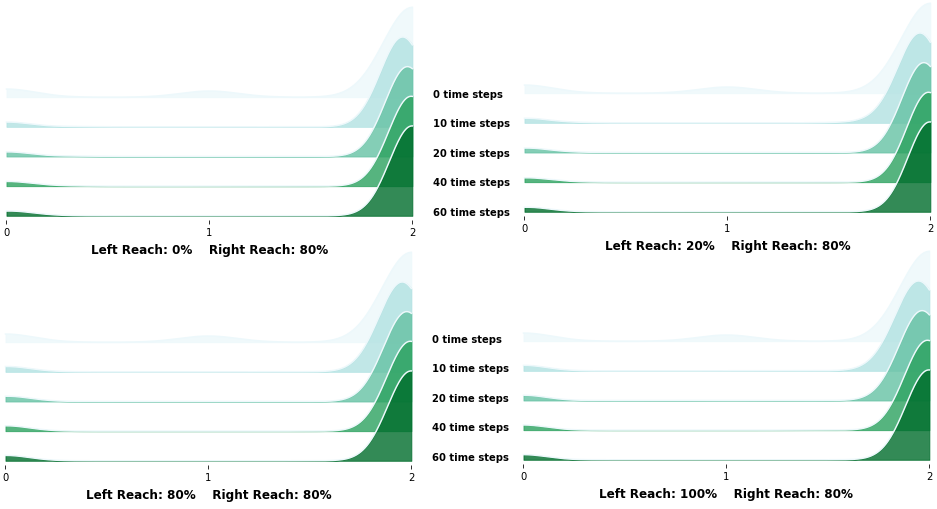


FIGURE 9. A population with *skeptical* initial beliefs over 60 time steps with a right mega-influencer of strong reach ($p_R = 0.8$) and a left mega-influencer of varying reach ($p_L = 0, 0.2, 0.8$,and 1).

6. Conclusion

The most interesting scenario among those we have simulated is that of a population that initially leans towards accepting the vaccine, with some vaccine skeptics. The data suggest that this may have been the situation in the state of Alabama, for instance, when Covid-19 vaccines were first developed.

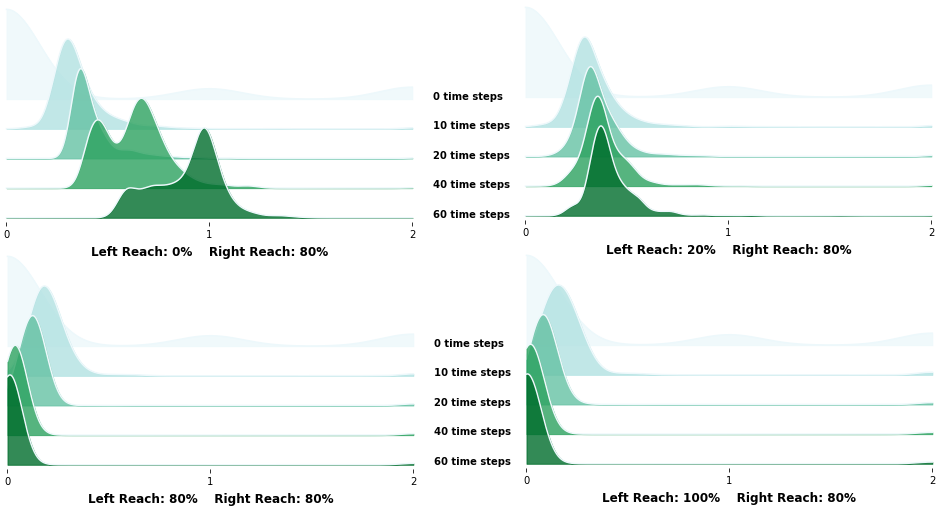


FIGURE 10. A population with *skewed* initial beliefs (such as Montgomery County, Alabama) over 60 time steps with a right mega-influencer of strong reach ($p_R = 0.8$) and a left mega-influencer of varying reach ($p_L = 0, 0.2, 0.8$,and 1).

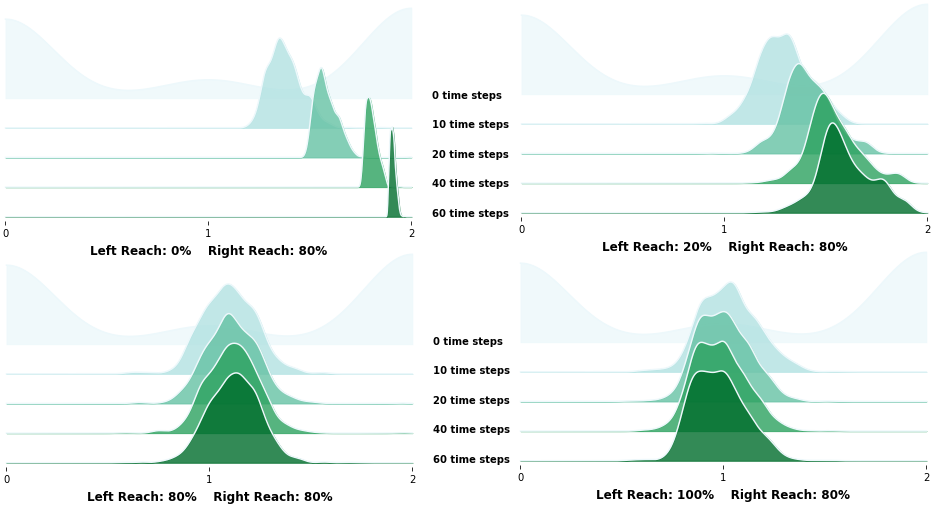


FIGURE 11. A population with *symmetric* initial beliefs over 60 time steps with a right mega-influencer of strong reach ($p_R = 0.8$) and a left mega-influencer of varying reach ($p_L = 0, 0.2, 0.8$,and 1).

Remarkably, in such a situation, if there were no mega-influencers, tight vaccine-accepting consensus would emerge in our model. However, a vaccine-hesitant mega-influencer who reaches a large fraction of those who are not strongly vaccine-accepting to begin with can cause a dramatic shift towards vaccine hesitancy. This is true even under our very conservative assumption that a mega-influencer counts, for those who listen to them, no more than a single friend, colleague, or neighbor would count.

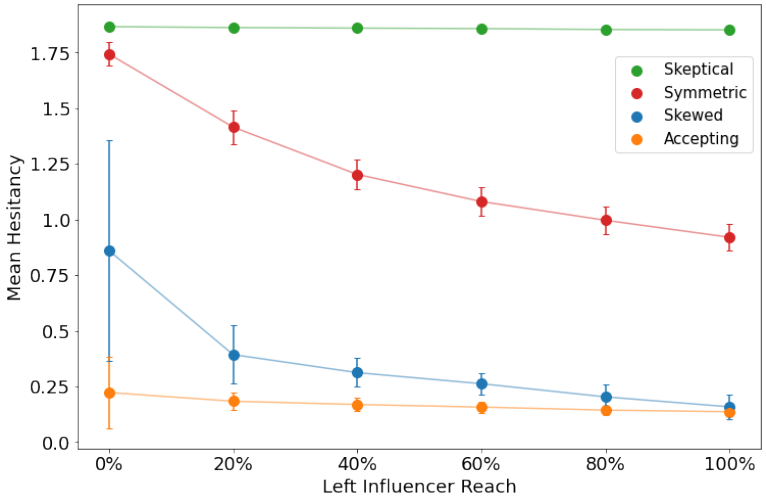


FIGURE 12. Mean belief at stopping as a function of left influencer reach for four different initial conditions. Averaged over 50 runs with errors bars indicating 1 standard deviation. The *Heavily Skewed Accepting* and *Skeptical* populations begin with initial vaccine hesitancy estimates of Multnomah County, OR and its reflection. The *Slightly Skewed Accepting* population begins with initial vaccine hesitancy estimates of Montgomery County, AL.

A competing vaccine-accepting mega-influencer reaching all those who are not strongly vaccine-hesitant already can counter-act this effect. In fact, it is surprisingly easy for the vaccine-accepting mega-influencer to reverse the trend: They do not need to match the reach of the vaccine-hesitant mega-influencer to succeed.

However, while the vaccine-accepting mega-influencer can shift the mean population view back towards vaccine acceptance, a much greater spread in views is always seen when there are two mega-influencers, in comparison with a population in which there are none.

We summarize our main points.

- Powerful mega influence from the right can move even a strongly-vaccine *accepting* population over to the right. Just talking to the people around you (friends, family, etc.) is not enough to effect widespread community belief change.
- You can stop mass-migration to the right, but you may not be able to stop broadening of the belief distribution, and this is especially noticeable in initially *skewed* populations.

Social media make spatial proximity less important, but tend to make people interact more selectively with the like-minded as both a consequence of social and algorithmic behavioral drivers [34]. One could attempt to model this effect by changing parameters in our model, making spatial proximity less important, and making like-mindedness more important, in determining the probabilities p_{uv}.

Our results also suggest future work on the dependence on the parameters b and ϵ; note that smaller values of b and ϵ will require replacing the discrete initial distributions (beliefs of 0, 1, or 2) by a continuous distribution. Further, we intend to work on scalable sampling algorithms for combining triangles into counties and counties into states. We plan to attempt to understand how time steps in our model map onto real time. Another feature to be added

to the model in the future would be the effects of central interventions such as government or workplace vaccine mandates. The connection between beliefs and Covid-19 is also seen in the study of the spread of misinformation [11]; these notions could also be incorporated into our model.

7. Acknowledgments

The authors wish to thank the Data Intensive Studies Center at Tufts University for generous support through a SEED Grant.

References

[1] A. Sirbu, V. Loreto, V. D. P. Servedio and F. Tria. *Opinion dynamics: models, extensions and external effects*. 2016, https://arxiv.org/abs/1605.06326.

[2] R. van der Hofstad. *Random Graphs and Complex Networks, Volume 1*. Cambridge Series in Statistical and Probabilistic Mathematics, 2017.

[3] J. Lorenz. *Continuous opinion dynamics under bounded confidence: A survey*. Int. J. Modern Phys. C, vol. 18, no. 12, pp. 1819–1838, 2007.

[4] Centers for Disease Control and Prevention. *Vaccine Hesitancy for COVID-19: County and local estimates*. https://data.cdc.gov/Vaccinations/Vaccine-Hesitancy-for-COVID-19-County-and-local-es/q9mh-h2tw, Last Accessed: December 8, 2021.

[5] Lengyel, B., Varga, A., Ságvári, B., Jakobi, Á., and Kertész, J. *Geographies of an online social network*. PloS one 10.9 (2015): e0137248.

[6] Centers for Disease Control and Prevention. *COVID-19 Vaccinations in the United States, County*. https://data.cdc.gov/Vaccinations/COVID-19-Vaccinations-in-the-United-States-County/8xkx-amqh, Last Accessed: December 8, 2021.

[7] Centers for Disease Control and Prevention. *Trends in Number of COVID-19 Vaccinations in the US*. https://covid.cdc.gov/covid-data-tracker/#vaccination-trends, Last Accessed: December 8, 2021.

[8] Centers for Disease Control and Prevention. *COVID-19 Vaccination*. https://www.cdc.gov/coronavirus/2019-ncov/vaccines/distributing/about-vaccine-data.html, Last Accessed: December 8, 2021.

[9] B. P. Murthy, N. Sterrett, D. Weller, et al. *Disparities in COVID-19 Vaccination Coverage Between Urban and Rural Counties – United States*. December 14, 2020–April 10, 2021. MMWR Morb Mortal Wkly Rep 2021;70, pp. 759– 764. DOI: http://dx.doi.org/10.15585/mmwr.mm7020e3externalicon.

[10] C. Simas and H. J. Larson. *Overcoming vaccine hesitancy in low-income and middle-income regions*. Nat Rev Dis Primers 7, 41 (2021). https://doi.org/10.1038/s41572-021-00279-w

[11] N. Rabb, L. Cowen, J. P. de Ruiter, M. Scheutz, M. *Cognitive cascades: How to model (and potentially counter) the spread of fake news*. Plos one, 17(1), e0261811.

[12] A.L.Beatty, N.D. Peyser, X.E. Butcher, et al. *Analysis of COVID-19 Vaccine Type and Adverse Effects Following Vaccination*. JAMA Netw Open. 2021;4(12):e2140364. doi:10.1001/jamanetworkopen.2021.40364

[13] J. L. Kriss, L. E. Reynolds, A. Wang, et al. *COVID-19 Vaccine Second-Dose Completion and Interval Between First and Second Doses Among Vaccinated Persons – United States*. December 14, 2020 – February 14, 2021. MMWR Morb Mortal Wkly Rep 2021;70:389–395. DOI: http://dx.doi.org/10.15585/mmwr.mm7011e2.

[14] R. Hegselmann and U. Krause. *Opinion dynamics and bounded confidence models, analysis, and simulation*. Journal of Artificial Societies and Social Simulation, vol. 5, 2002.

[15] R. Hegselmann and U. Krause. *Opinion dynamics under the influence of radical groups, charismatic leaders, and other constant signals: A simple unifying model*. Networks & Heterogeneous Media 10.3 (2015): 477.

[16] F. Chung and L. Lu. *The average distances in random graphs with given expected degrees*. Proceedings of the National Academy of Sciences (PNAS), 99(25), pp. 15879 – 15882, 2002.

[17] F. Chung and L. Lu. *Connected components in random graphs with given expected degree sequences.* Annals of Combinatorics, 6(2), pp. 125 – 145, 2002.
[18] F. Chung and L. Lu. *The average distance in a random graph with given expected degrees.* Internet Mathematics, 1(1), pp. 91 – 113, 2004.
[19] K. Bringmann, R. Keusch, and J. Lengler. *Sampling Geometric Inhomogeneous Random Graphs in Linear Time.* 2016, https://arxiv.org/abs/1511.00576.
[20] J-D. Mathias, S. Huet, and G. Deffuant. *Bounded confidence model with fixed uncertainties and extremists: The opinions can keep fluctuating indefinitely.* Journal of Artificial Societies and Social Simulation 19.1 (2016): 6.
[21] M. Barthélemy. *Spatial networks.* Physics reports 499.1-3 (2011): 1-101.
[22] U. Krause. *Soziale Dynamiken mit vielen Interakteuren. Eine Problemskizze, in Proc. Modellierung Simul. von Dynamiken mit vielen interagierenden Akteuren.* 1997, pp. 37–1.
[23] U. Krause. *A discrete nonlinear and non-autonomous model of consensus formation.* Communications in difference equations, 2000 (2000), pp. 227 – 236.
[24] J. Lorenz. *A stabilization theorem for continuous opinion dynamics.* Physica A, vol. 355, no. 1, pp. 217–223, 2005.
[25] J. Lorenz. *Consensus strikes back in the Hegselmann-Krause model of continuous opinion dynamics under bounded confidence.* J. Artif. Societies Social Simul., vol. 9, no. 1, 2006.
[26] E. Ben-Naim. *Rise and fall of political parties.* Europhys. Lett., vol. 69, no. 5, pp. 671–676, 2005.
[27] S. Fortunato, V. Latora, A. Pluchino and A. Rapisarda. *Vector opinion dynamics in a bounded confidence consesnus model.* Int. J. Modern Phys. C, vol. 16, pp. 1535–1551, Oct. 2005.
[28] D. Urbig. *Attitude dynamics with limited verbalisation capabilities.* J. Artif. Societies Social Simul., vol. 6, no. 1, 2003.
[29] F. Gargiulo and Y. Gandica. *The role of homophily in the emergence of opinion controversies.* arXiv preprint (2016) arXiv:1612.05483.
[30] Department of Health and Human Services. *ASPE Predictions of Vaccine Hesitancy for COVID-19 Vaccines by Geographic and Sociodemographic Features.* Methodological Description, Assistant Secretary for Planning and Evaluation Issue Brief, June 17, 2021, https://aspe.hhs.gov/sites/default/files/migrated_legacy_files//200821/vaccine-hesitancy-COVID-19-Methodology.pdf, Last Accessed: Oct. 20, 2021.
[31] T. Beleche, J. Ruhter A. Kolbe, J. Marus, L. Bush and B. Sommers. *COVID-19 Vaccine Hesitancy: Demographic Factors, Geographic Patterns, and Changes Over Time.* Assistant Secretary for Planning and Evaluation Issue Brief, Department of Health and Human Services, May, 2021, https://aspe.hhs.gov/sites/default/files/migrated_legacy_files//200816/aspe-ib-vaccine-hesitancy.pdf, Last Accessed: Oct. 13, 2021.
[32] R.I.M. Dunbar. *Do online social media cut through the constraints that limit the size of offline social networks?.* Royal Society Open Science 3.1 (2016): 150292.
[33] S. J. Hardima and L. Katzir. *Estimating clustering coefficients and size of social networks via random walk.* Proceedings of the 22nd international conference on World Wide Web. 2013.
[34] M. Cinelli, G. De Francisci Morales, A. Galeazzi, W. Quattrociocchi and M. Starnini. *The echo chamber effect on social media.* Proceedings of the National Academy of Sciences Mar 2021, 118 (9) e2023301118; DOI: 10.1073/pnas.2023301118
[35] M. Workman. *An empirical study of social media exchanges about a controversial topic: Confirmation bias and participant characteristics.* Journal of Media in Society, 7 (1), 2018, pp. 381–400.

(Anna Haensch) Tufts University, Data Intensive Studies Center
Email address, Corresponding author: anna.haensch@tufts.edu

(Natasa Dragovic) Tufts University, Department of Mathematics
Email address: natasa.dragovic@tufts.edu

(Christoph Börgers) Tufts University, Department of Mathematics
Email address: christoph.borgers@tufts.edu

(Bruce Boghosian) Tufts University, Department of Mathematics
Email address: bruce.boghosian@tufts.edu